

Electronic Supplementary Information

**Energy gradient architected praseodymium chalcogenide
quantum dot solar cells: Towards unidirectionally funneling energy
transfer**

Xiao Jin^{a,§}, Weifu Sun^{b,§}, Shenglian Luo^{a,*}, Liping Shao^a, Jian Zhang^a, Xubiao Luo^a, Taihuei
Wei^c, Yuancheng Qin^a, Yinglin Song^{d,*}, Qinghua Li^{a,*}

^aKey Laboratory of Jiangxi Province for Persistent Pollutants Control and Resources Recycle,
Nanchang Hangkong University, Nanchang 330063, PR China

^bSchool of Aerospace, Mechanical and Mechatronic Engineering, The University of Sydney,
New South Wales 2006, Australia

^cDepartment of Physics, National Chung-Cheng University, Chia-Yi 621, Taiwan, Republic of
China

^dDepartment of Physics, Harbin Institute of Technology, Harbin 150001, PR China

[§]These authors contributed equally to this work.

*e-mail: qhli@hqu.edu.cn; shenglianluo@163.com; ylsong@hit.edu.cn

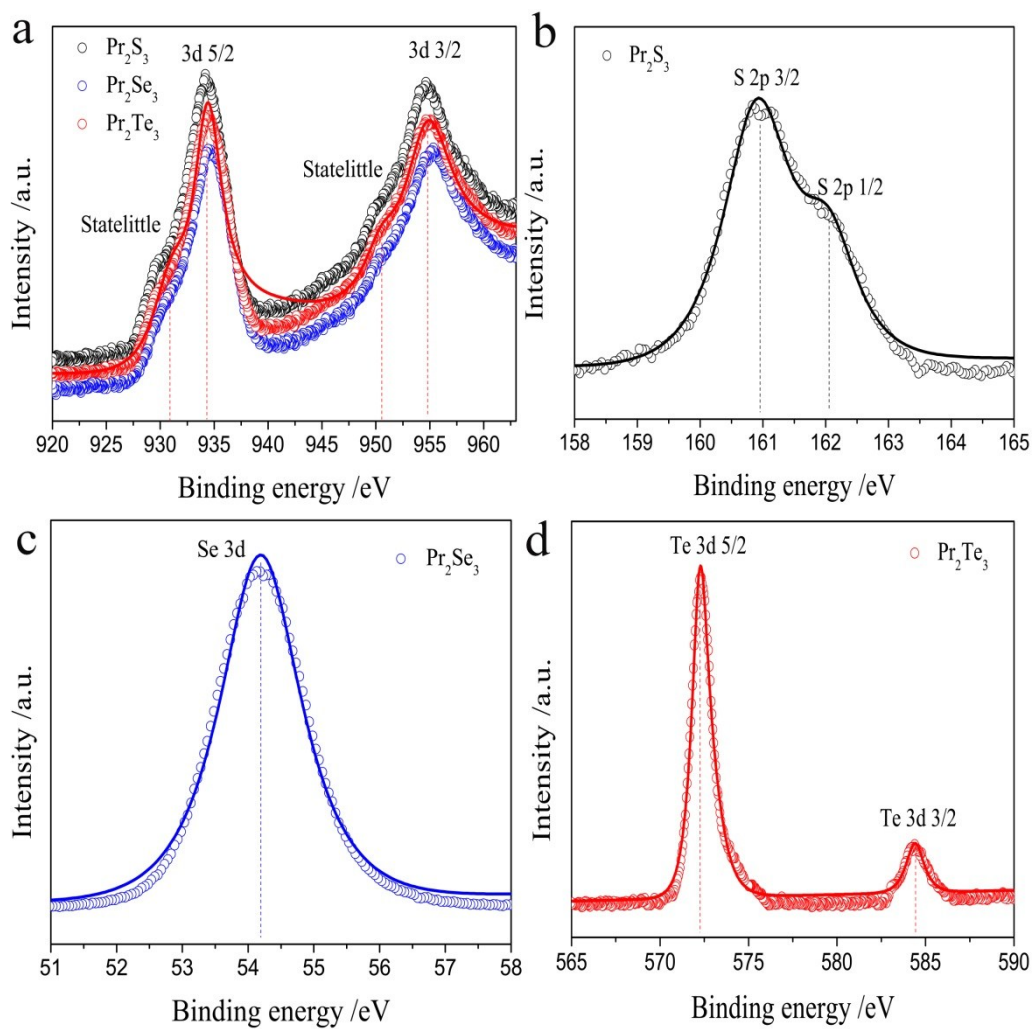


Fig. S1 XPS spectra of Pr 3d for $\text{Pr}_2(\text{S}, \text{Se}, \text{Te})_3$ QDs (a), XPS spectra of S 3d for Pr_2S_3 QDs (b), Se 3d for Pr_2Se_3 QDs (c) and Te 3d for Pr_2Te_3 QDs (d).

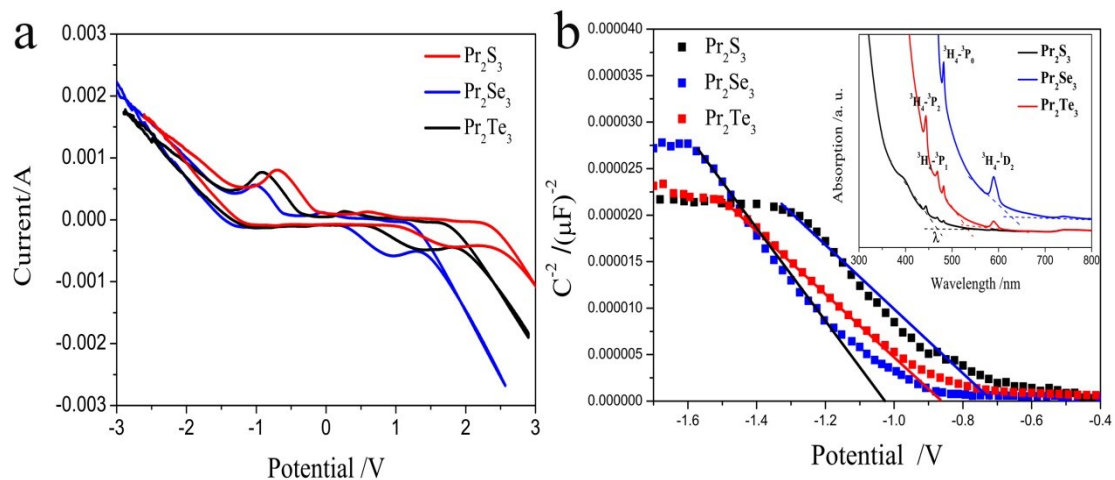


Fig. S2 (a) The CV characteristics of the QD films in acetonitrile containing 0.1 M tetramethylammonium perchlorate in dimethylformamide at a sweep rate of 50 mV s⁻¹; (b) Mott-Schottky plots of the different QD films at 1 kHz in 0.05 M Na₂SO₄ aqueous solution and the insert highlights the UV-vis absorption spectra of the three films.

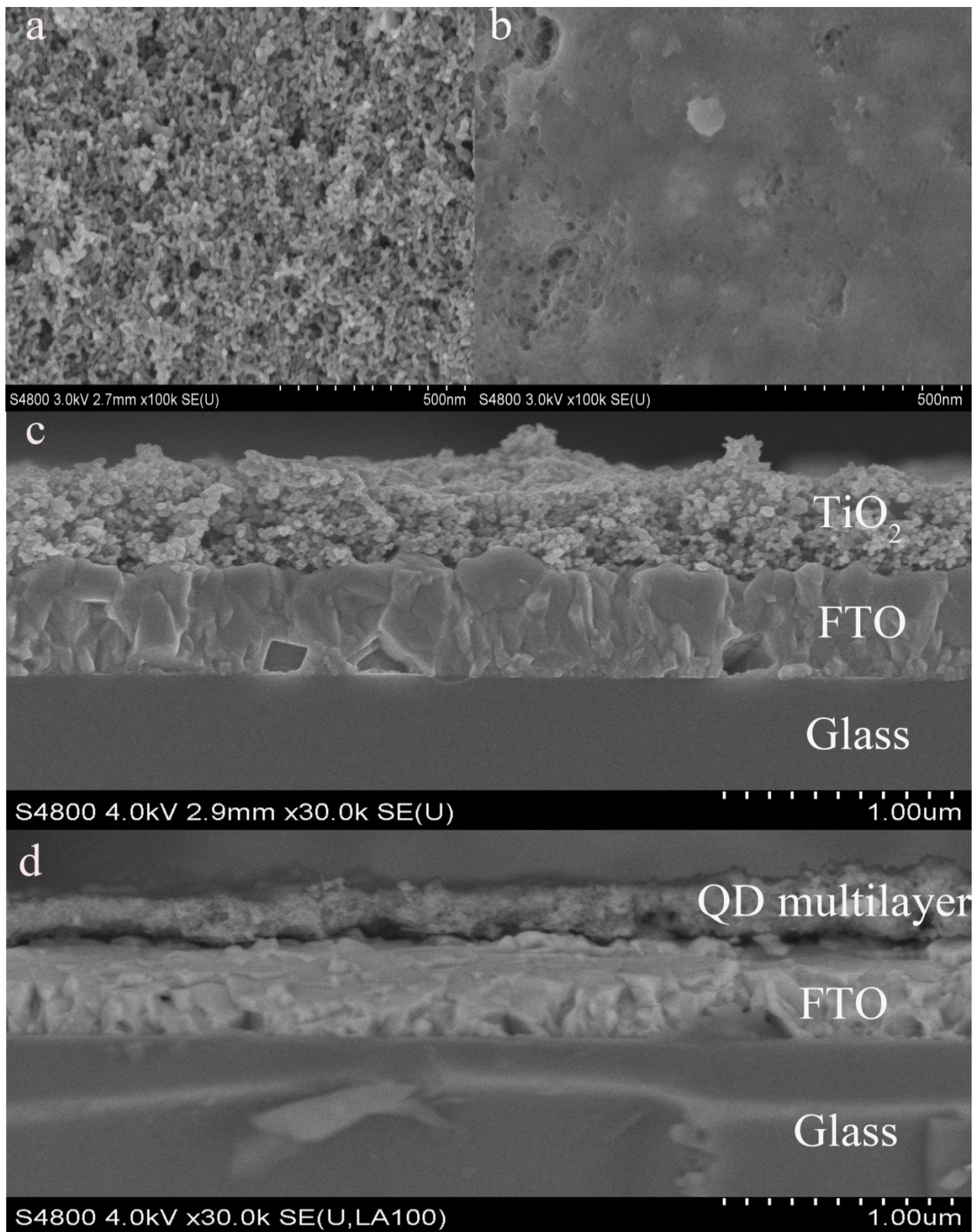


Fig. S3 SEM images of the bare TiO₂ (a) and Pr₂Se₃/Pr₂Te₃/Pr₂S₃/TiO₂ films, cross-sectional SEM images of TiO₂ (c) and the QD multilayers (d).

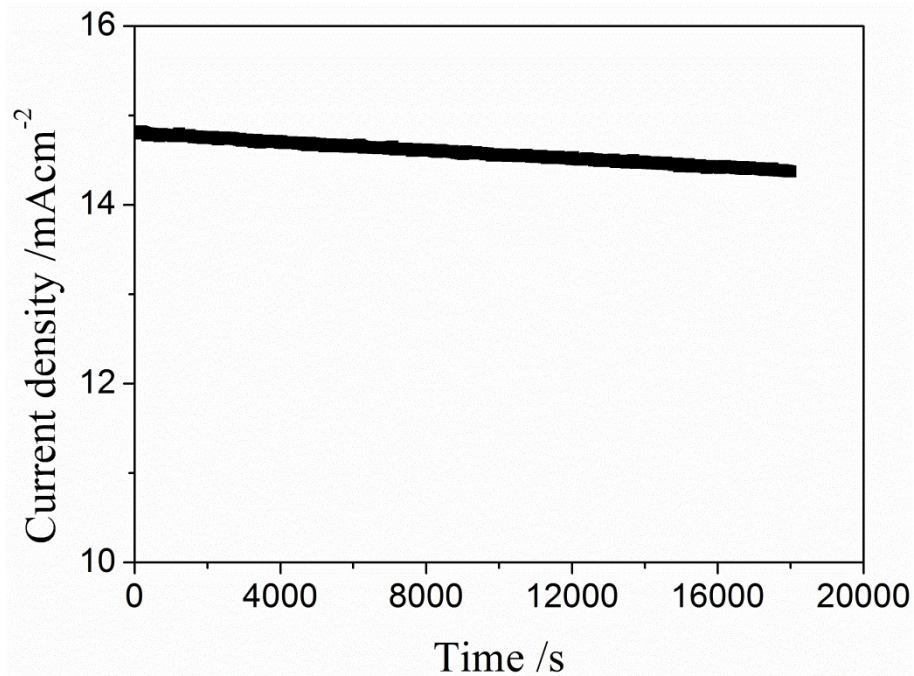


Fig. S4. Photocurrent density of the assembled $\text{Pr}_2\text{Se}_3/\text{Pr}_2\text{Te}_3/\text{Pr}_2\text{S}_3/\text{TiO}_2$ quadruple-stack QDSC was recorded with irradiation over 5 h under prolonged irradiation of 100 mWcm^{-2} .

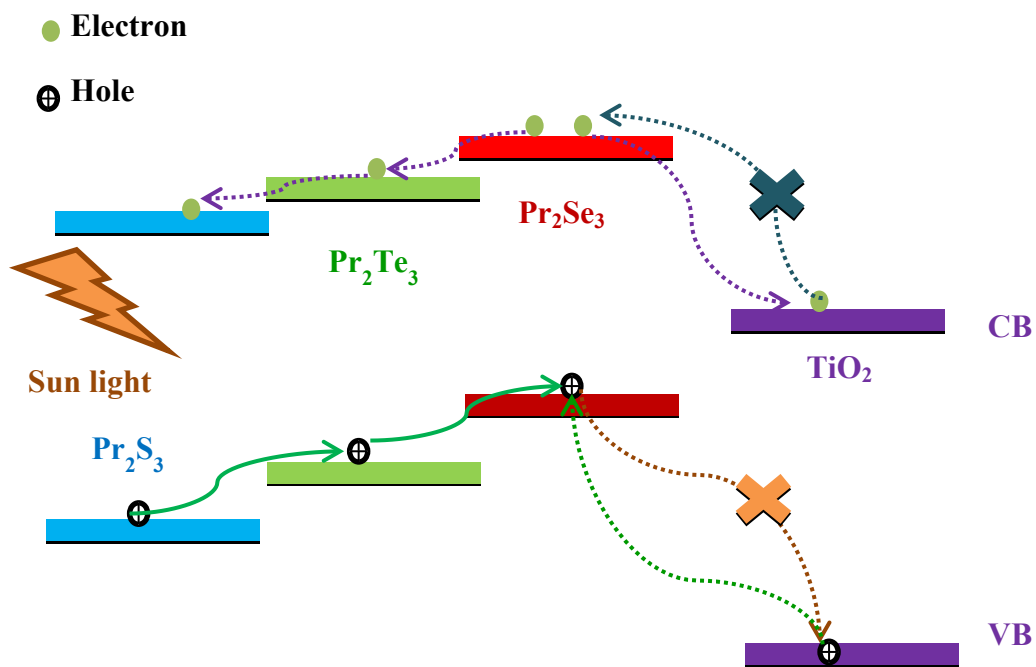


Fig. S5. Energy band diagram of the $\text{Pr}_2\text{S}_3/\text{Pr}_2\text{Te}_3/\text{Pr}_2\text{Se}_3/\text{TiO}_2$ heterojunction and the schematic diagram displaying charge transfer for photogeneration in the QDs.

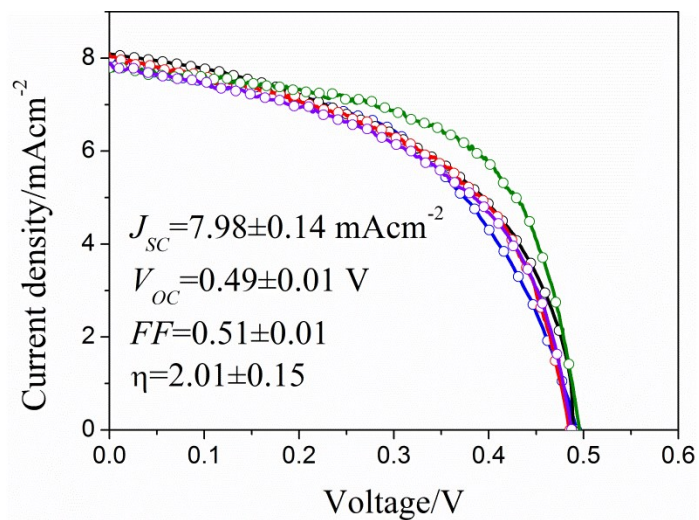


Fig. S6. J - V characteristics of $\text{Pr}_2\text{S}_3/\text{Pr}_2\text{Te}_3/\text{Pr}_2\text{Se}_3/\text{TiO}_2$ QDSC under AM1.5G solar simulated illumination.

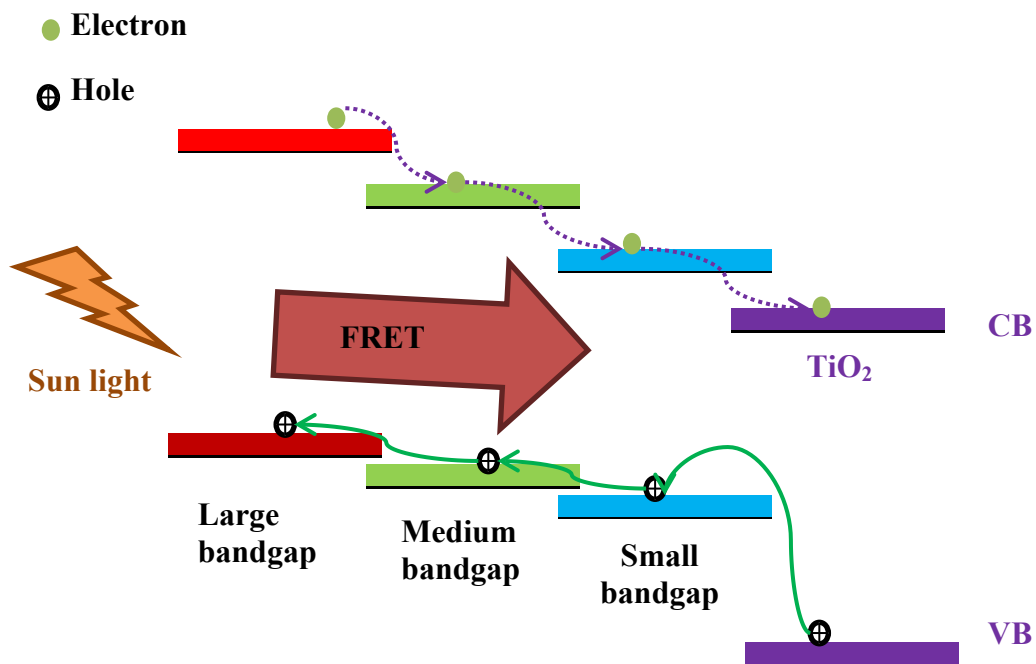


Fig. S7. The schematic diagram of an ideal multilayer displaying the energy levels, charge transfer, and FRET.

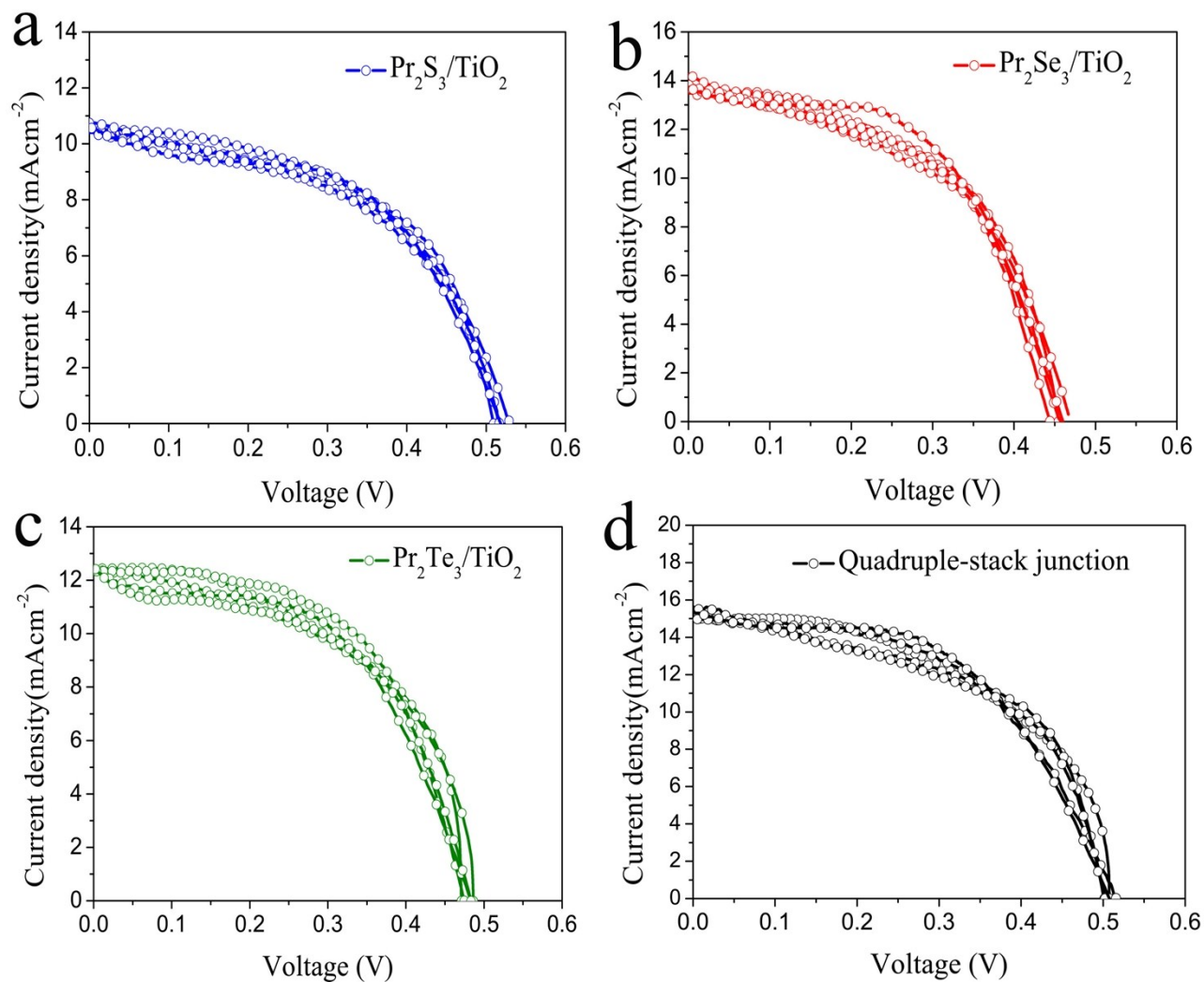


Fig. S8. J - V characteristics of $\text{Pr}_2\text{S}_3/\text{TiO}_2$ (a) $\text{Pr}_2\text{Se}_3/\text{TiO}_2$ (b) $\text{Pr}_2\text{Te}_3/\text{TiO}_2$ and $\text{Pr}_2\text{Se}_3/\text{Pr}_2\text{Te}_3/\text{Pr}_2\text{S}_3/\text{TiO}_2$ QDSCs in AM1.5G solar simulated light.